planes typical of cardiac muscle fibres were detected within the iPSC-CM grafts, but not in the infarcted myocardium of the sham-treated rats (Figure 3); albeit reflection intensity was generally much less than that obtained from the remote myocardium. Furthermore, in iPSC-CM hearts cyclic changes in myosin mass-transfer to actin with regular changes in myofilament lattice spacing were evident (Figure 4); similar to that previously reported by us for *in situ* beating rat hearts (20). Importantly, the shift in myosin mass to actin of the iPSC-CMs was synchronous with LV pressure increase during the start of systole on a beat-by-beat basis (Figure 5). The decrease in intensity ratio from end-diastole through early-systole was approximately linearly related to LV pressure development (Figure 5, lower panel). Hence, significant cyclic systolic myosin head transfer to actin filaments, and therefore force-developing cross-bridges were detected within the grafts. Notably, implanted iPSC-CM sheets produced consistent reflections, but the same sheets fresh from culture did not reveal any reflections.

Consistent with the findings in the synchrotron study, myosin and actin were well aligned in the cytoplasm of the Dsred-positive transplanted iPSC-CMs, which were present in the surface of the rat heart, assessed by immunohistolabeling (Figure 6A). In contrast, Dsred-negative native CMs were rarely found in the border and infarct areas which were assessed in the synchrotron study. These findings indicate that the *in situ* X-ray diffraction pattern originated from the transplanted iPSC-CMs, suggesting that regular actin-myosin cross-bridge motion had occurred in the transplanted iPSC-CMs in the rat heart.

Phenotypic and morphological fate of the transplanted iPSC-CM in the heart

Phenotype, morphology and microstructure of the transplanted iPSC-CM, which might be modulated following transplantation into the cardiac tissue, were then histologically analyzed by using immunoconfocal microscopy and electron microscopy. Dsrred-positive transplanted

iPSC-CMs showed myosin-positive sarcomeres at 14 days after transplantation (Figure 6A and B). The sarcomeres consisted of myosin and sarcomeric actin. Although the transplanted iPSC-CMs expressed Cx43 at 14 days, the distribution of Cx43 was scarce, and did not clearly show the typical intercalated disks between the transplanted iPSC-CMs (Figure 6C).

In vitro iPSC-CMs showed typical sarcomeric structures in cardiac myocytes with immature, less dense mitochondria (Figure 6D). On the other hand, clear desmosomes were generated between the iPSC-CMs at 3 days after transplantation, while the mitochondria showed more mature structure compared to that prior to the transplantation. At 7 days, mitochondria showed mature structure, whereas the sarcomeric structure or the number of mitochondria was not as dense as those in the native CMs (Figure 6E and F). This indicates that the transplanted iPSC-CMs by the cell-sheet method might have established electrical/mechanical integrity with the native heart. In addition, maturity in the structure and functionality of the iPSC-CMs progressed after the transplantation into the heart.

DISCUSSION

We demonstrated here that the amount of VEGF and HGF released by iPSC-CMs was not significantly different from that of the same number of fibroblasts, *in vitro*. Transplantation of the iPSC-CM cell-sheets of mouse origin into the nude rat heart that was subjected to MI better preserved LV function and ARI, compared to that of the fibroblasts. Daily electrical mapping of the heart surface uncovered that transplantation of the iPSC-CM induced multiple ectopic excitations over the cell-sheet implanted area for the initial 2 days, and subsequently ectopic excitations disappeared. In *in vivo* synchrotron radiation small-angle scattering studies, the transplanted iPSC-CMs displayed regularly contracting actin-myosin cross-bridge interactions, similar to that recorded in the native cardiomyocytes of the remote myocardium of the same hearts. Immunohistologically, the transplanted iPSC-CMs, which were equipped with myosin-positive sarcomeres in the cytoplasm, formed Cx43-gap-junction with the native cardiomycytes, while electronmicroscopically, the transplanted iPSC-CMs were equipped with immature sarcomeres and mitochondria, compared to the native cardiomyocytes.

The mechanisms underlying the global functional recovery by iPSC-CM transplantation include 1) that transplanted iPSC-CMs survived and showed synchronized contraction *in vivo* as proven by the diffraction analyses, 2) that transplanted iPSC-CMs were equipped with fully developed sarcomeres *in vivo* and these cells might connect with the recipient myocardium, and 3) that there is functional integration of the transplanted iPSC-CMs into the native myocardium to produce direct mechanical contribution to cardiac function. The direct effects of the transplanted cells were studied chiefly by histological assessment of the excised cardiac tissues, which were examined for the presence and integration of the transplanted cells into the native cardiac tissue, but not the functionality of the transplanted cells. For the first time, *in vivo* scans dissected contractile motion of the

transplanted cells by X-ray diffraction techniques using synchrotron radiation. Only X-ray diffraction using synchrotron radiation is able to detect rapid transient shifts in myosin mass most likely attributable to strong cross-bridge formation from relatively few muscle fibres within small regions (0.2 mm x 0.2 mm) (12,20). Myosin mass transfer in the first phase of systole in normal myocardial fibres is directly correlated with global LV force development (13). This feature has enabled us to investigate cardiomyocyte function within pin point regions of the graft, the infarct-borderzone and infarct-remote myocardium in heart failure rats. In this study, contractile motion of the Dsred-labeled iPSC-CMs was clearly dissected from the native cardiomyocytes by the synchrotron study, as the cells were transplanted as a sheet form on the heart surface. In the absence of living native cardiomyocytes beneath the graft it is reasonable to conclude that strong cross-bridge formation of the iPSC-CMs contributed to force development, albeit much reduced compared to remote myocardium. In addition, electrical and functional integration of the transplanted iPSC-CMs in the heart was revealed by electrical mapping and echocardiography, supplemented with histological studies, indicating that contraction of each transplanted iPSC-CMs was transferred into the native cardiac motion, at least in part, contributing to the functional recovery of MI heart.

Other possible mechanisms underlying the functional recovery by the transplantation of iPSC-CM cell-sheets might include "paracrine effects" of the transplanted cells on the native heart (19). In fact, this study revealed that the known paracrine factors, such as VEGF or HGF, were released *in vitro* from the iPSC-CMs as from the fibroblasts, while fibroblasts were proven here not to be differentiated into functional cardiomyocytes after transplantation into the heart. Of note, functional recovery was produced in the iPSC-CMs-transplanted hearts but not in the fibroblast-transplanted hearts, despite similar release of the paracrine factors between those two cell-sources. Although these data would be insufficient to determine the magnitude of the "paracrine effects" by the iPSC-CMs therapy, it is suggested

that functional recovery by the iPSC-CMs transplantation might be chiefly caused by mechanical effects of the transplanted cells, and partly by the paracrine effects. Further basic studies are warranted for magnitude and/or durability of paracrine effects by this treatment.

The transplanted graft was integrated into the cardiac tissue beneath the epicardial layer, in particular, the epicardial layer of the infarct and infarct-border territory in this study. In contrast, it seemed that integration of the transplanted cells crossing the epicardium was less prominent in the remote myocardium from the infarct territory (data not shown). We thus consider that integration of the cell-sheet was determined by the microenvironment of the native cardiac tissue and that ablation of the epicardium prior to the cell-sheet transplantation may enhance the integration of the cell-sheet graft (10). In addition, thorough immunohistolabelling and electron microscopy studies showed abundant expression of connexin43 in the graft but rarely identify the gap junction formation between the graft and the native tissue. We consider that presence of a few gap junctions might be enough to transfer electrical current from the native tissue to the grafted cells.

In this study, the transplanted iPSC-CMs showed an "immature" structure, which was not equipped with dense sarcomeric structure and mitochondrial arrangement, as shown in the immunohistolocial and electron microscopy analysis. This was also evident in the lower reflection intensities obtained from sheet-derived CMs compared to native remote myocardium. Importantly, this study indicates that maturity of iPSC-CMs may progress after transplantation into the heart, though quantitative analysis of the "maturity" of the transplanted cells is needed. The functionality of each transplanted iPSC-CMs, in particular its contractility, is the most important factor in determining the therapeutic effects of this treatment. We also showed that the maturity of *in vitro* differentiated iPSC-CMs is variable according to the origin, the cell-line and the culture protocol, and therefore specific regimens used in culture protocols, such as mechanical stretching in the cell-preparation, mimicking the

in vivo environment, might be useful in enhancing the maturation *in vitro* (4,23). One can consider that cell-cell connections between the "immature" cardiomyocytes transplanted into the LV and the native LV cardiomyocytes is likely to produce electrical instability in the LV myocardium resulting in the induction of ventricular arrhythmias. In fact, multiple ectopic excitations appeared in the cell-transplanted area and gradually decreased. Possible causes of the prominent occurrence of premature ventricular contractions in the iPSC-CMs-treated animals would include ectopic excitation directly produced by the transplanted and integrated "immature" iPSC-CMs, or macro/micro re-entries generated by cell transplantation-induced myocardial heterogeneity (1). Although this study failed to dissect the exact cause of the premature contraction, we consider that heterogeneity in the native cardiac tissue would be the main cause, since frequency of the premature contractions was stable for 7 days despite the progressive electrical integration of the graft during this period as in the Figure 1A. While it is unclear that maturation of the transplanted iPSC-CMs is associated with the progressive electrical stability in the LV myocardium in this study, more efficient culture-protocols to enhance maturity of iPSC-CMs, and thereby maximize the therapeutic effects and minimize the arrhythmogenicity of this treatment warrant further investigation.

A limitation of this study may be that we used different species for the iPSC origin and the recipient animal. Interspecies differences may influence functional and electrical integration of the transplanted cells into the recipient native heart. However, the mouse and rat share important proteins related to cell-cell connections and sarcomere structure in the heart (18). The data here therefore are unlikely to be affected by a use of such a xeno-transplantation model. Another limitation could be use of a single iPSC cell-line. As it has been shown that the cell-line is one of the important variable factors that determines the fundamental behavior of iPSCs and their derivatives (22), further studies are warranted to establish an efficient culture protocol to produce the cells that have a consistent quality

towards clinical application. In addition, quantitative study of the transplanted cell-survival in the heart would provide further information regarding this treatment.

In conclusion, transplanted iPSC-CMs in a cell-sheet form displayed regularly contracting actin-myosin cross-bridge interactions in the heart surface with synchronous contraction with the native cardiac tissue, contributing to global functional recovery from ischemic heart injury in the rat. High-flux synchrotron X-ray diffraction offers a promising potential as an *in vivo* cellular and molecular level modality for evaluating transplanted iPSC-CM function. Finally, it is important to develop culture protocols to enhance functionality of the iPSC-CMs for successful clinical application of this treatment.

FUNDING

This work was supported by the Research Center Network for Realization of Regenerative Medicine managed by Centers for Clinical Application Research on Specific Disease/Organ and funded by Japan Science and Technology Agency, and the International Synchrotron Access Programme (IA111) managed by the Australian Synchrotron and funded by the Australian Government.

CONFLICT OF INTEREST

The authors declare no conflicts of interest.

REFERENCES

1. Fukushima, S.; Coppen, S. R.; Lee, J.; Yamahara, K.; Felkin, L. E.; Terracciano, C. M. N.; Barton, P. J. R.; Yacoub, M. H.; Suzuki, K. Choice of cell-delivery route for skeletal myoblast transplantation for treating post-infarction chronic heart failure in rat. PLoS One 3(8):e3071; 2008.
2. Fukushima, S.; Sawa, Y.; Suzuki, K. Choice of cell-delivery route for successful cell transplantation therapy for the heart. Future Cardiol. 9(2):215-227; 2013.
3. Fukushima, S.; Varela-Carver, A.; Coppen, S. R.; Yamahara, K.; Felkin, L. E.; Lee, J.; Barton, P. J. R.; Terracciano, C. M. N.; Yacoub, M. H.; Suzuki, K. Direct intramyocardial but not intracoronary injection of bone marrow cells induces ventricular arrhythmias in a rat chronic ischemic heart failure model. Circulation 115(17):2254-2261; 2007.
4. Kamakura, T.; Makiyama, T.; Sasaki, K.; Yoshida, Y.; Wuriyanghai, Y.; Chen, J.; Hattori, T.; Ohno, S.; Kita, T.; Horie, M. and others. Ultrastructural maturation of human-induced pluripotent stem cell-derived cardiomyocytes in a long-term culture. Circ. J. 77(5):1307-1314; 2013.
5. Kawamura, M.; Miyagawa, S.; Miki, K.; Saito, A.; Fukushima, S.; Higuchi, T.; Kawamura, T.; Kuratani, T.; Daimon, T.; Shimizu, T. and others. Feasibility, safety, and therapeutic efficacy of human induced pluripotent stem cell-derived cardiomyocyte sheets in a porcine ischemic cardiomyopathy model. Circulation 126(11 suppl 1):S29-S37; 2012.
6. Memon, I. A.; Sawa, Y.; Fukushima, N.; Matsumiya, G.; Miyagawa, S.; Taketani, S.; Sakakida, S. K.; Kondoh, H.; Aleshin, A. N.; Shimizu, T. and others. Repair of impaired myocardium by means of implantation of engineered autologous myoblast sheets. J.Thorac. Cardiovasc. Surg. 130(5):1333-1341; 2005.

CT-1353 Cell Transplantation Early Epub; provisional acceptance 12/04/2014

7. Miki, K.; Uenaka, H.; Saito, A.; Miyagawa, S.; Sakaguchi, T.; Higuchi, T.; Shimizu, T.; Okano, T.; Yamanaka, S.; Sawa, Y. Bioengineered myocardium derived from induced pluripotent stem cells improves cardiac function and attenuates cardiac remodeling following chronic myocardial infarction in tats. Stem Cells Transl. Med. 1(5):430-437; 2012.

8. Miyagawa, S.; Saito, A.; Sakaguchi, T.; Yoshikawa, Y.; Yamauchi, T.; Imanishi, Y.; Kawaguchi, N.; Teramoto, N.; Matsuura, N.; Iida, H. and others. Impaired myocardium regeneration with skeletal cell sheets—A preclinical trial for tissue-engineered regeneration therapy. Transplantation 90(4):364-372; 2010.

9. Miyagawa, S.; Sawa, Y.; Sakakida, S.; Taketani, S.; Kondoh, H.; Memon, I. A.; Imanishi, Y.; Shimizu, T.; Okano, T.; Matsuda, H. Tissue cardiomyoplasty using bioengineered contractile cardiomyocyte sheets to repair damaged myocardium: Their integration with recipient myocardium. Transplantation 80(11):1586-1595; 2005.

10. Muraoka, I.; Takatsuki, M.; Sakai, Y.; Tomonaga, T.; Soyama, A.; Hidaka, M.; Hishikawa, Y.; Koji, T.; Utoh, R.; Ohashi, K. and others. Transplanted fibroblast cell sheets promote migration of hepatic progenitor cells in the incised host liver in allogeneic rat model. J Tissue Eng. Regen. Med. [Epub ahead of print]; 2013.

11. Nakagawa, M.; Koyanagi, M.; Tanabe, K.; Takahashi, K.; Ichisaka, T.; Aoi, T.; Okita, K.; Mochiduki, Y.; Takizawa, N.; Yamanaka, S. Generation of induced pluripotent stem cells without Myc from mouse and human fibroblasts. Nat Biotech 26(1):101-106; 2008.

12. Pearson, J. T.; Shirai, M.; Ito, H.; Tokunaga, N.; Tsuchimochi, H.; Nishiura, N.; Schwenke, D. O.; Ishibashi-Ueda, H.; Akiyama, R.; Mori, H. and others. In Situ Measurements of Crossbridge Dynamics and Lattice Spacing in Rat Hearts by X-Ray Diffraction: Sensitivity to Regional Ischemia. Circulation 109(24):2976-2979; 2004.

13. Pearson, J. T.; Shirai, M.; Tsuchimochi, H.; Schwenke, D. O.; Ishida, T.; Kangawa, K.;

Suga, H.; Yagi, N. Effects of Sustained Length-Dependent Activation on In Situ Cross-Bridge Dynamics in Rat Hearts. Biophys. J. 93(12):4319-4329; 2007.

14. Ptaszek, L. M.; Mansour, M.; Ruskin, J. N.; Chien, K. R. Towards regenerative therapy for cardiac disease. Lancet 379(9819):933-942; 2012.
15. Sawa, Y.; Miyagawa, S.; Sakaguchi, T.; Fujita, T.; Matsuyama, A.; Saito, A.; Shimizu, T.; Okano, T. Tissue engineered myoblast sheets improved cardiac function sufficiently to discontinue LVAS in a patient with DCM: report of a case. Surg Today 42(2):181-184; 2012.
16. Shiba, Y.; Fernandes, S.; Zhu, W.-Z.; Filice, D.; Muskheli, V.; Kim, J.; Palpant, N. J.; Gantz, J.; Moyes, K. W.; Reinecke, H. and others. Human ES-cell-derived cardiomyocytes electrically couple and suppress arrhythmias in injured hearts. Nature 489(7415):322-325; 2012.
17. Shirai, M.; Schwenke, D. O.; Tsuchimochi, H.; Umetani, K.; Yagi, N.; Pearson, J. T. Synchrotron radiation imaging for advancing our understanding of cardiovascular function. Circ. Res. 112(1):209-221; 2013.
18. Stagg, M. A.; Coppen, S. R.; Suzuki, K.; Varela-Carver, A.; Lee, J.; Brand, N. J.; Fukushima, S.; Yacoub, M. H.; Terracciano, C. M. N. Evaluation of frequency, type, and function of gap junctions between skeletal myoblasts overexpressing connexin43 and cardiomyocytes: relevance to cell transplantation. FASEB J. 20(6):744-746; 2006.
19. Suzuki, K.; Murtuza, B.; Smolenski, R. T.; Sammut, I. A.; Suzuki, N.; Kaneda, Y.; Yacoub, M. H. Cell transplantation for the treatment of acute myocardial infarction using vascular endothelial growth factor–expressing skeletal myoblasts. Circulation 104(suppl 1):I-207-I-212; 2001.
20. Toh, R.; Shinohara, M.; Takaya, T.; Yamashita, T.; Masuda, S.; Kawashima, S.; Yokoyama, M.; Yagi, N. An X-ray diffraction study on mouse cardiac cross-bridge

function in vivo: Effects of adrenergic β-stimulation. Biophys. J. 90(5):1723-1728; 2006.

21. Yagi, N.; Shimizu, J.; Mohri, S.; Araki, J. i.; Nakamura, K.; Okuyama, H.; Toyota, H.; Morimoto, T.; Morizane, Y.; Kurusu, M. and others. X-ray diffraction from a left ventricular wall of rat heart. Biophys. J. 86(4):2286-2294; 2004.
22. Yoshida, Y.; Yamanaka, S. iPS cells: A source of cardiac regeneration. J. Mol. Cell. Cardiol. 50(2):327-332; 2011.
23. Yu, T.; Miyagawa, S.; Miki, K.; Saito, A.; Fukushima, S.; Higuchi, T.; Kawamura, M.; Kawamura, T.; Ito, E.; Kawaguchi, N. and others. In vivo differentiation of induced pluripotent stem cell-derived cardiomyocytes. Circ. J. 77(5):1297-1306; 2013.

FIGURE LEGENDS

Figure 1. **(A)** Representative image of electrical current over the iPSC-CMs-transplanted heart surface in one cardiac cycle, visualized by 64-channel mapping system at day 2, day 3 and day 7 (n=4 each). Multiple ectopic excitations which were present at day 2 and day 3 were not detected at day 7. **(B)** Frequency of the VPC was calculated by continuous telemetric electrocardiogram monitoring (n=4 each). It appeared slightly greater in the iPSC-CMs-transplanted rats compared to the sham-operated rats, though there was no significant difference.

Figure 2. **(A)** Activation recovery interval (ARI), measured by daily 64-channel mapping studies, was significantly greater in the the iPSC-CMs (iPS) group compared to the other groups from the day 3 onwards (n=4 each). **(B)** Left ventricular ejection fraction (LVEF), measured by daily transthoracic echocardiography, was significantly greater in the iPSC-CMs group compared to the other groups from the day 3 onwards (n=6 each).

Figure 3. Small-angle X-ray scattering analysis of the red-circled area in the iPSC-CMs-transplanted heart at day 14 **(A)** showed appearance of the 1,0 and 1,1 equatorial reflections at the end-systolic phase **(B** and **C)**. In contrast, blue-circled scar tissue of the sham-operated heart **(D)** showed 1,0 reflections only at the end-systolic phase **(E** and **F)**. n=4 each.

Figure 4. Observed 1,0 reflection intensity change, calculated myosin interfilament spacing ($d_{1,0}$) and myosin mass transfer index (equatorial intensity ratio $I_{1,0}/I_{1,1}$) over several consecutive cardiac cycles in an iPSC-CM sheet of a transplant heart. Regular loop like

relations between myosin mass transfer were evident.

Figure 5. Observed 1,0 reflection intensity change, calculated myosin interfilament spacing ($d_{1,0}$), myosin mass transfer index (equatorial intensity ratio $I_{1,0}/I_{1,1}$) and simultaneously acquired LV pressure acquired over several consecutive cardiac cycles in an iPSC-CM sheet of a transplant heart. Significant 1,0 myosin reflections were only evident for part of the cardiac cycle due to heart movement. When significant actin-myosin reflections were evident the shift in myosin mass towards actin (decrease in intensity ratio) coincided with the rapid increase in LV pressure during systole showing synchronized contraction of the iPSC-CMs in the sheet. Arrows indicate timing of end diastole.

Figure 6. Dsred-labelled transplanted iPSC-CMs expressed clear myosin-positive sarcomeres as shown in the representative confocal micrograph **(A)**. The sarcomere of the transplanted iPSC-CMs consisted of myosin and sarcomeric actin **(B)**. Distribution of the Cx43 did not show the typical intercalated disks in the transplanted iPSC-CMs **(C)**. The scale bar indicates ten micrometers. The iPSC-CMs *in vitro* showed the cardiac myocyte-like sarcomeres with less dense mitochondrial structures (arrow) as shown in the representative electron micrograph **(D)**. *In vivo* transplanted iPSC-CMs showed clear desmosome structure between the cells (arrow heads, **E**). Mitochondria of the transplanted iPSC-CMs *in vivo* gradually showed a dense structure at day 3 **(E)** and then at day 7 **(F)**. n=5 each.

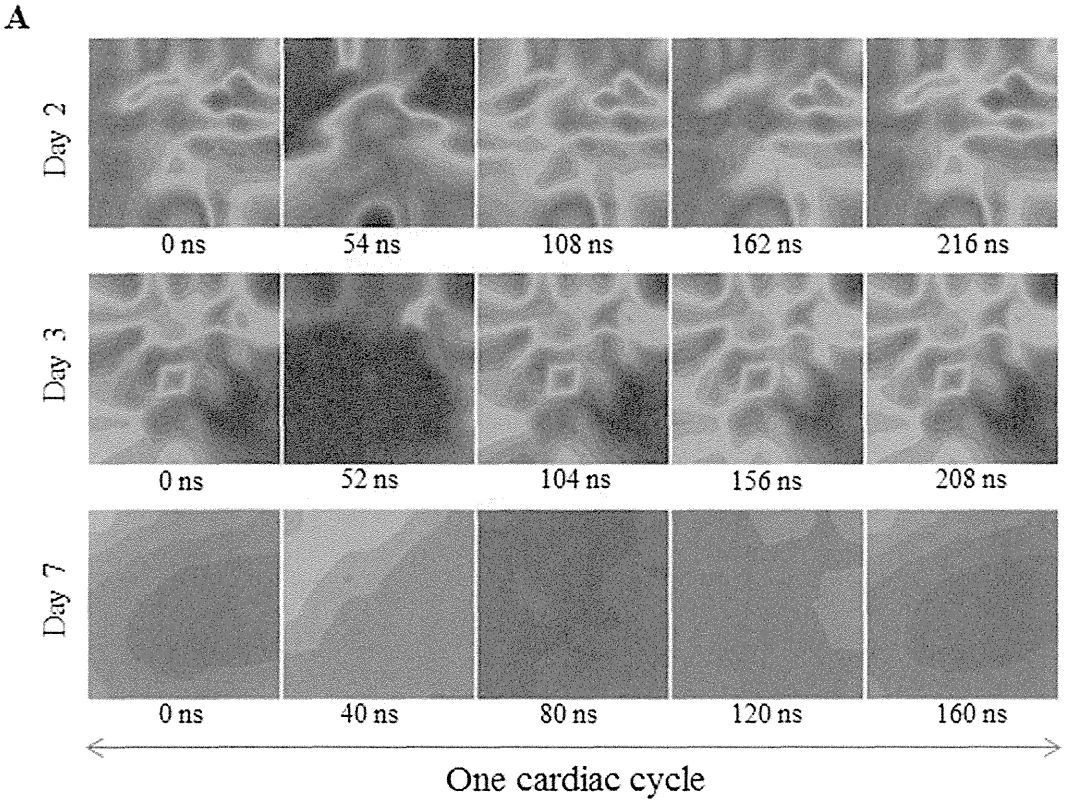

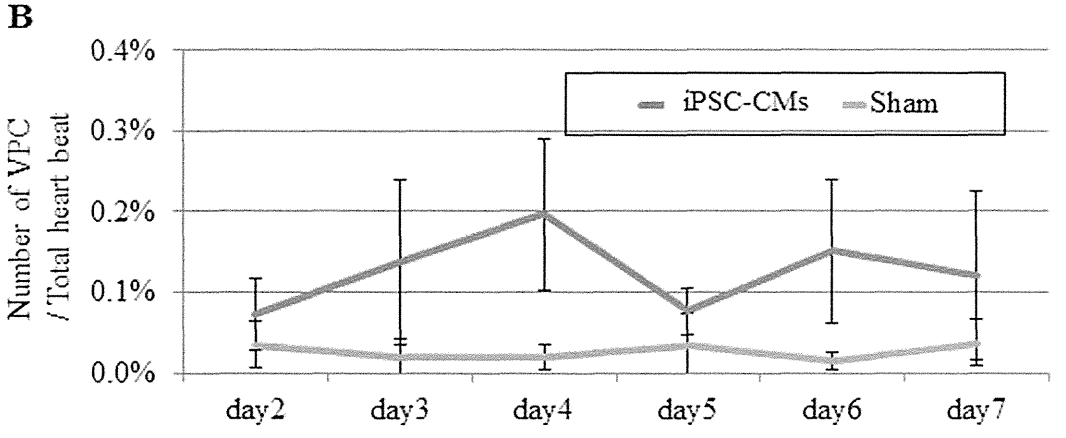

Figure 1

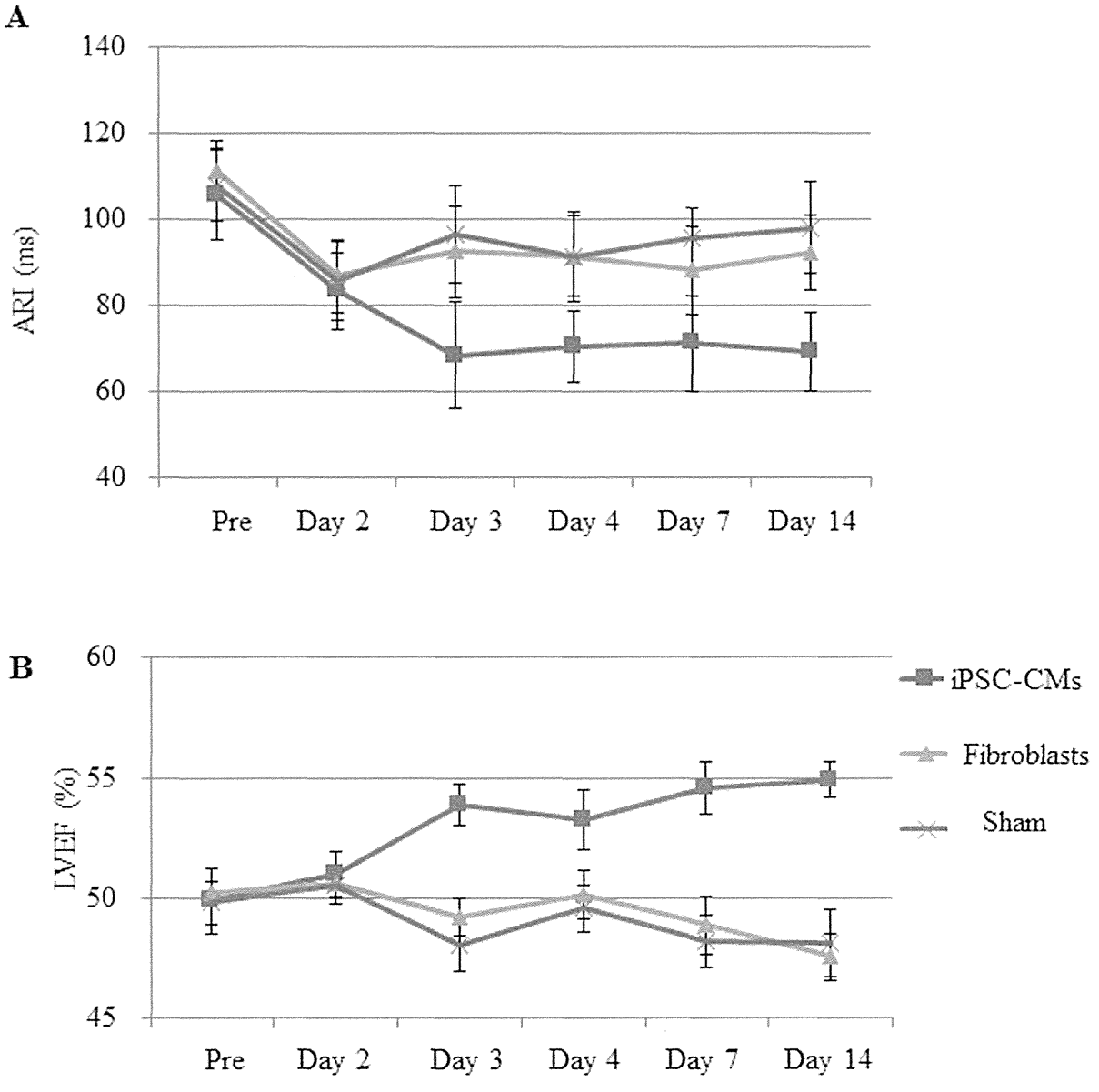

Figure 2

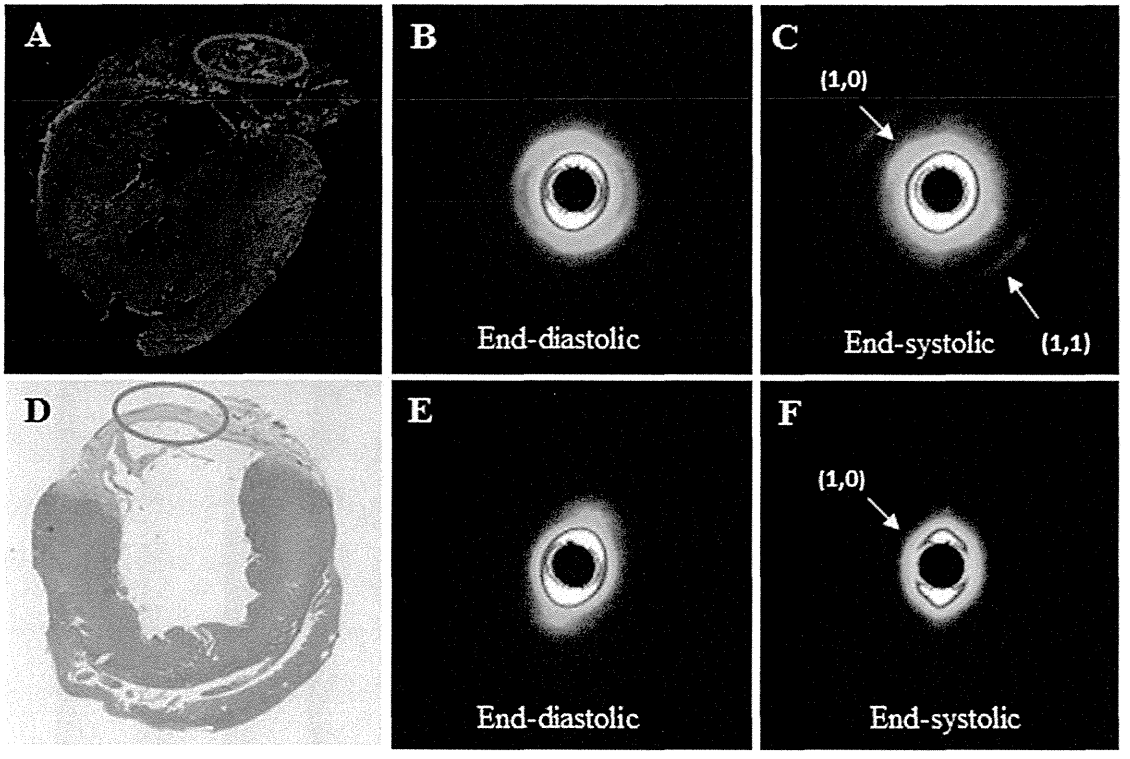

Figure 3

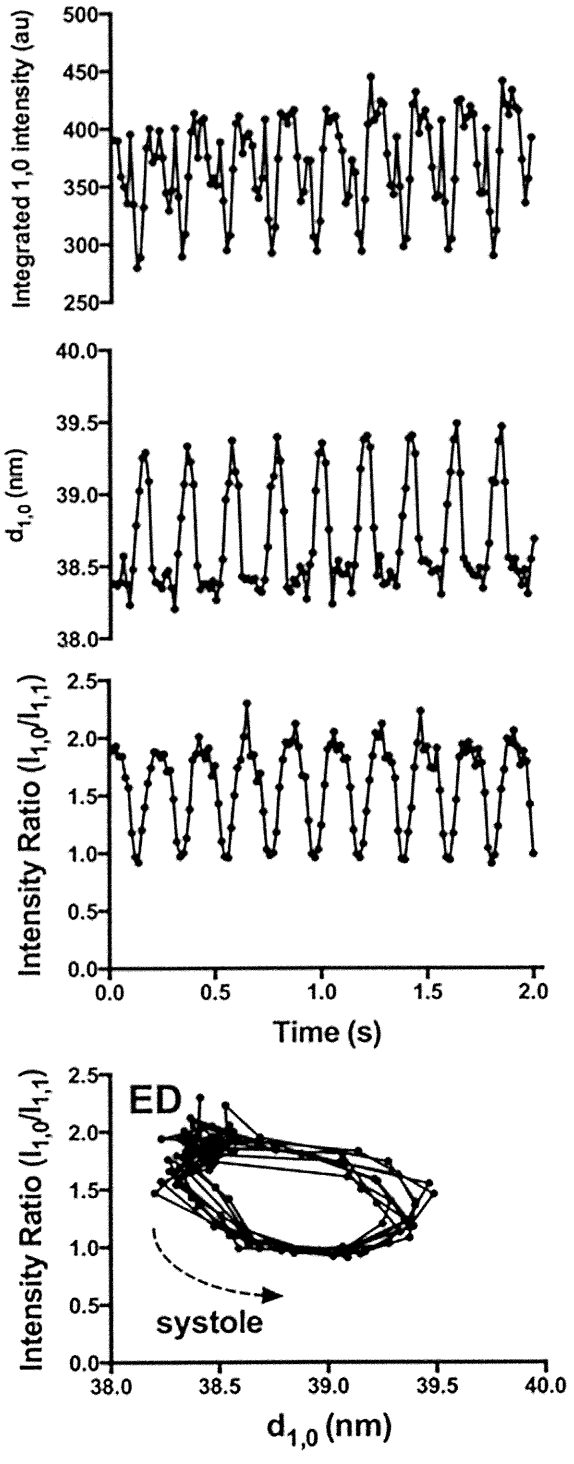

Figure 4

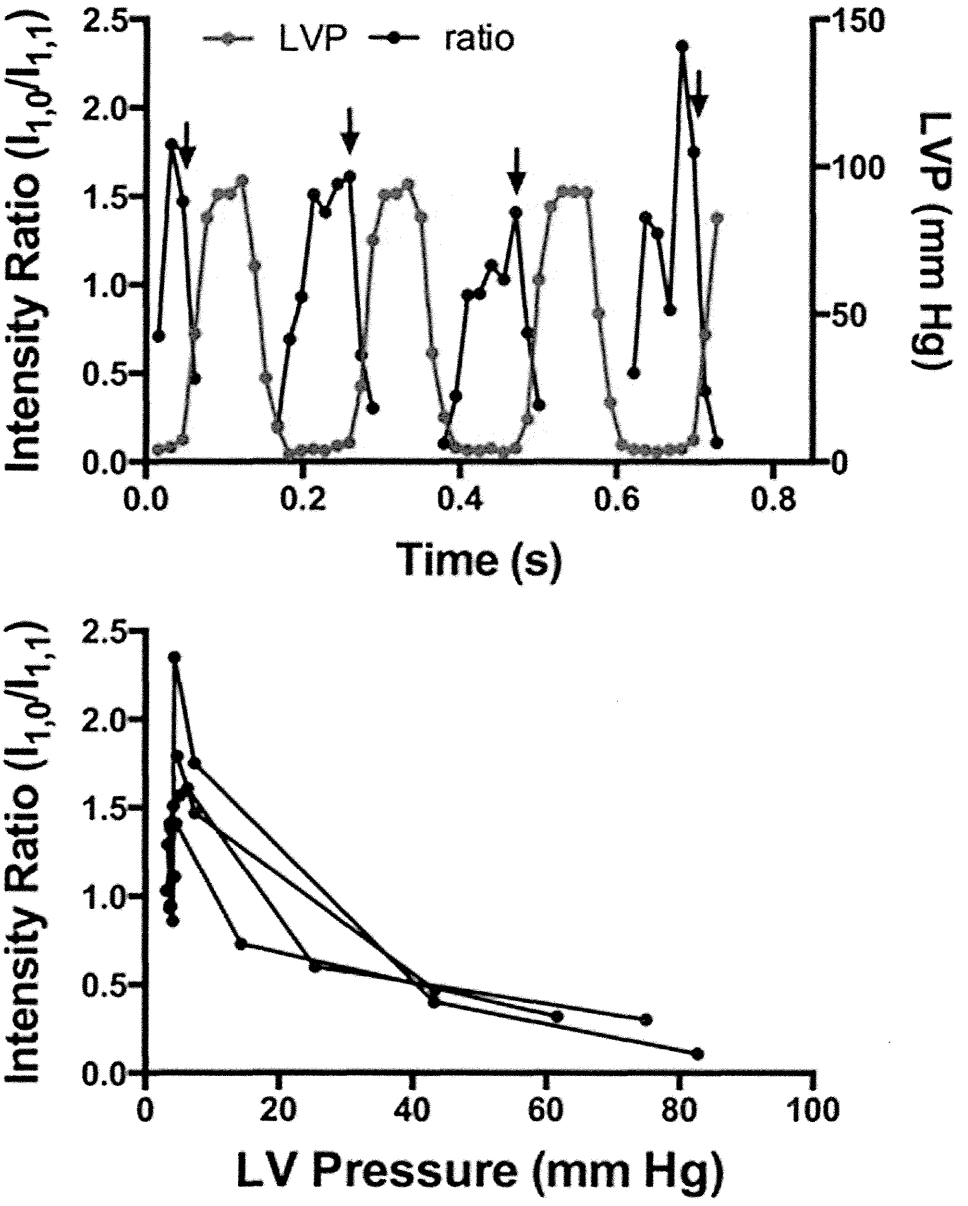

Figure 5

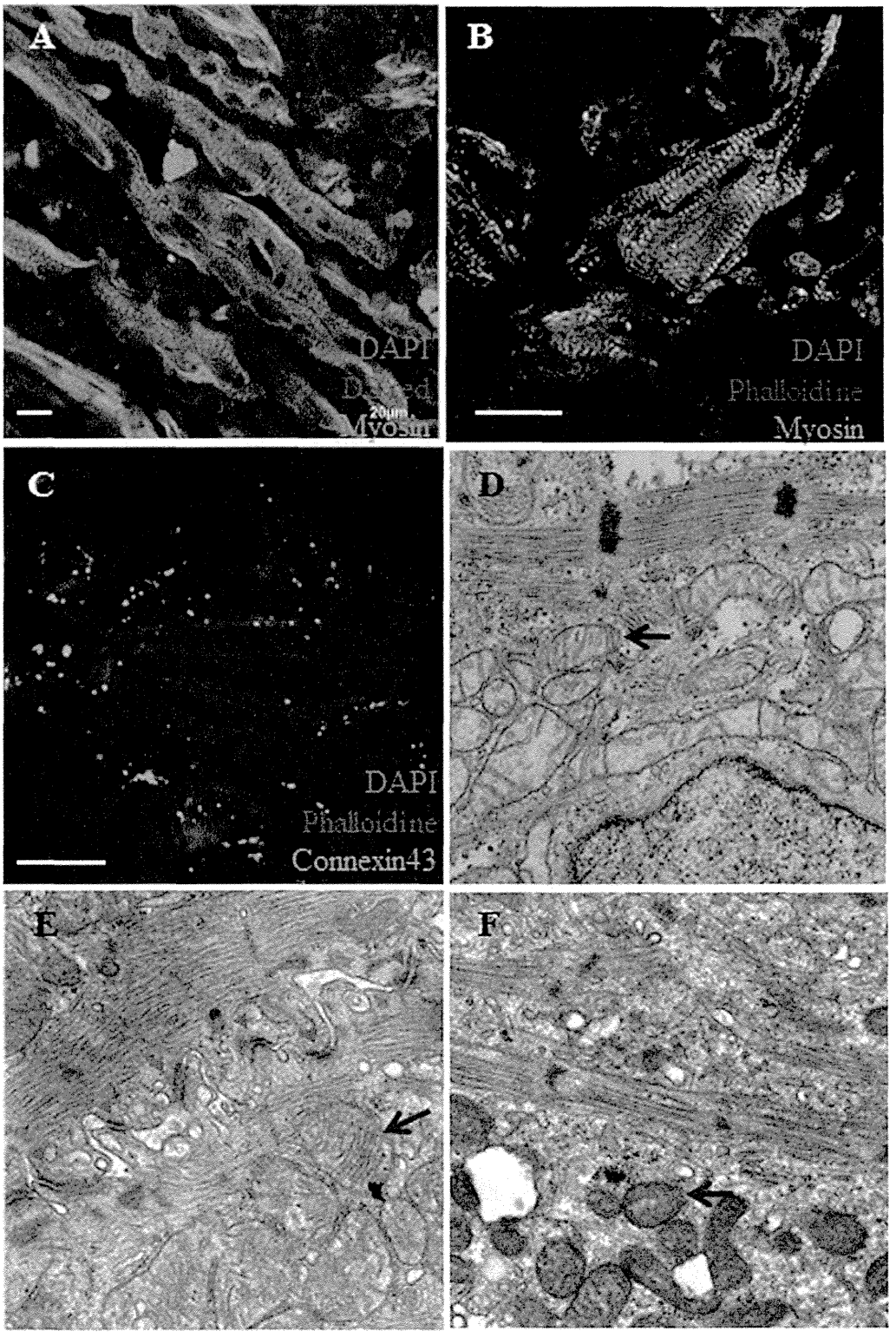

Figure 6